Science Advances
AAAS

advances.sciencemag.org/cgi/content/full/6/8/eaax2926/DC1

Supplementary Materials for

Phenotypic plasticity of carbon fixation stimulates cyanobacterial blooms at elevated CO_2

Xing Ji, Jolanda M. H. Verspagen, Dedmer B. Van de Waal, Björn Rost, Jef Huisman*

*Corresponding author. Email: j.huisman@uva.nl

Published 19 February 2020, *Sci. Adv.* **6**, eaax2926 (2020)
DOI: 10.1126/sciadv.aax2926

This PDF file includes:

Section S1. Description of bicarbonate uptake of *Microcystis* PCC 7941

Bicarbonate uptake rates of *Microcystis* PCC 7941 showed a pattern that differs from *Microcystis* PCC 7806 and most other cyanobacteria and green algae investigated so far (Fig. S1, C and D). Instead of standard Michaelis-Menten kinetics, bicarbonate uptake rates of *Microcystis* PCC 7941 increased sharply to maximum levels at low to intermediate bicarbonate concentrations (4 – 100 µmol L^{-1}), but then decreased and leveled off to a lower uptake rate at high bicarbonate concentrations (>500 µmol L^{-1}). Therefore, we extended the Michaelis-Menten equation with a hyperbolic inhibition term to capture the asymptotic decrease of its bicarbonate uptake rate at high bicarbonate concentrations

$$V_{HCO3} = \left(\frac{U_{max,HCO3}[\mathrm{HCO_3^-}]}{K_{1/2,HCO3} + [\mathrm{HCO_3^-}]}\right)\left(\frac{B_{1/2,HCO3}}{B_{1/2,HCO3} + [\mathrm{HCO_3^-}]} + h\right) \quad (1.1)$$

Here, $U_{max,HCO3}$ is the hypothetical maximum bicarbonate uptake rate in the absence of inhibition, $K_{1/2,HCO3}$ is the half-saturation constant, $B_{1/2,HCO3}$ is the half-saturation inhibition constant (i.e., the concentration where inhibition is half of the maximum inhibition rate), and *h* describes the maximum uptake rate realized at high bicarbonate concentrations as fraction of the hypothetical maximum uptake rate. When we fitted this model to the data, we found that the half-saturation inhibition constant $B_{1/2,HCO3}$ was very similar and in several replicates even identical to the half-saturation constant for uptake, $K_{1/2,HCO3}$. Therefore, we simplified the model accordingly, and fitted all bicarbonate uptake kinetics of *Microcystis* PCC 7941 to the following model

$$V_{HCO3} = \left(\frac{U_{max,HCO3}[\mathrm{HCO_3^-}]}{K_{1/2,HCO3} + [\mathrm{HCO_3^-}]}\right)\left(\frac{K_{1/2,HCO3}}{K_{1/2,HCO3} + [\mathrm{HCO_3^-}]} + h\right) \quad (1.2)$$

To compare maximum bicarbonate uptake rates among different species, we calculated the asymptotic maximum bicarbonate uptake rate realized by *Microcystis* PCC 7941 at high bicarbonate concentrations

$$V_{max,HCO3} = U_{max,HCO3}\, h \quad (1.3)$$

The results show that $V_{max,HCO3}$ of *Microcystis* PCC 7941 was 40% lower in cells acclimated to high pCO_2 than in cells acclimated to low pCO_2 (Fig. S1, C and D; Fig. 3B). A reduction of the maximum bicarbonate uptake rate at high pCO_2 was not observed in *Microcystis* PCC 7806, but is known from other cyanobacteria (Table 1 in the main text).

Section S2. Description of the mathematical model

Introduction

To predict the population dynamics of *Microcystis* at different pCO_2 levels, we developed a mathematical model that combines earlier theoretical and experimental work on phytoplankton growth under light-limited (*42*, *48*) and carbon-limited conditions (*11*, *36*). The model considers a well-mixed water column (in this case, a chemostat vessel) with a depth z running from 0 at the surface to z_{max} at the bottom. The model assumes eutrophic conditions, in which all nutrients are in ample supply and hence do not limit cyanobacterial growth. Population dynamics of the cyanobacteria are governed by the carbon balance, which depends on the light-driven uptake of CO_2 and bicarbonate and on carbon losses through respiration. Uptake of dissolved CO_2 and bicarbonate induces changes in pH, and uptake of nutrients also changes alkalinity. These changes in pH and alkalinity affect the dissolved CO_2 and bicarbonate concentrations, which in turn feed back on carbon uptake and growth of the cyanobacteria. The expanding cyanobacterial population also increases the turbidity of the water column, thereby diminishing light available for further photosynthesis and growth.

Population dynamics

Let B denote the population density of cyanobacteria. The population dynamics can be written as

$$\frac{dB}{dt} = \mu B - DB \tag{2.1}$$

where μ is the specific growth rate of the cyanobacteria as function of inorganic carbon and light availability, and D is the dilution rate of the chemostat.

Carbon uptake kinetics

We assume that the growth rate of cyanobacteria in nutrient-saturated waters is governed by their carbon balance. The carbon balance depends on gross uptake of CO_2 ($V_{CO2,\,gross}$) and bicarbonate (V_{HCO3}) and on losses of CO_2 by respiration (r). Hence, the specific growth rate is calculated as

$$\mu = \frac{1}{Q_C}\left(V_{CO2,gross} + V_{HCO3} - r\right) \tag{2.2}$$

where Q_C is the cellular carbon content. For notational convenience, we also define the net CO_2 uptake rate as $V_{CO2,net} = V_{CO2,gross} - r$.

Our model assumes that uptake rates of CO_2 and bicarbonate are increasing functions of the dissolved CO_2 and bicarbonate concentration according to Michaelis-Menten kinetics and are driven by the energy obtained from the light reactions of photosynthesis

$$V_{CO2,gross} = \left(\frac{V_{max,CO2,gross}[\mathrm{CO_2}]}{K_{1/2,CO2}+[\mathrm{CO_2}]}\right) P \quad (2.3)$$

$$V_{HCO3} = \left(\frac{V_{max,HCO3}[\mathrm{HCO_3^-}]}{K_{1/2,HCO3}+[\mathrm{HCO_3^-}]}\right) P \quad (2.4)$$

where $V_{max,CO2,\ gross}$ and $V_{max,HCO3}$ are the maximum uptake rates of CO_2 and bicarbonate, respectively, and $K_{1/2,CO2}$ and $K_{1/2,HCO3}$ are the half-saturation constants. For *Microcystis* PCC 7941, we extended equation (2.4) with an inhibition term to capture the asymptotic decrease of its bicarbonate uptake rate at high bicarbonate concentrations (see section S1 for details). Since carbon fixation requires energy from photosynthesis, carbon uptake rates also depend on photosynthetic activity and hence on light availability. Here, P is the relative photosynthetic activity of the cyanobacteria (with $0 \leq P \leq 1$) as further specified below.

Phenotypic plasticity of carbon uptake kinetics

Phenotypically plastic traits are assumed to adjust dynamically to the prevailing environmental conditions. Let x denote the value of a plastic trait (such as V_{max} and $K_{1/2}$). Dynamic changes of this trait value are described as

$$\frac{dx}{dt} = c(f[\mathrm{CO_2}] - x(t)) \quad (2.5)$$

where the function $f[CO_2]$ describes the acclimated trait value as function of the dissolved CO_2 concentration, $x(t)$ is the actual trait value at time t, and c is the acclimation rate. The function $f[CO_2]$ is replaced by $f[\mathrm{HCO_3^-}]$ for traits involved in bicarbonate uptake. Hence, the trait value is at equilibrium if it has converged to the acclimated trait value, i.e., if $x = f[CO_2]$.

The functions $f[CO_2]$ and $f[\mathrm{HCO_3^-}]$ can be interpreted as the reaction norms of the plastic traits involved in CO_2 and bicarbonate uptake, respectively. We assume that the reaction norms have an S-shaped form, bound between the physiological limits x_{low} and x_{high} (Fig. 1C). This S-shape is captured by logistic equations

$$f[\mathrm{CO_2}] = x_{low} + \frac{x_{high}-x_{low}}{1+\mathrm{e}^{-d_{CO2}\left(\log[\mathrm{CO_2}]-\log(S_{CO2})\right)}} \quad (2.6)$$

$$f[\mathrm{HCO_3^-}] = x_{low} + \frac{x_{high}-x_{low}}{1+\mathrm{e}^{-d_{HCO3}\left(\log[\mathrm{HCO_3^-}]-\log(S_{HCO3})\right)}} \quad (2.7)$$

where d_{CO2} and d_{HCO3} represent the steepness of the logistic reaction norms, and S_{CO2} and S_{HCO3} are the CO_2 and bicarbonate concentration at the inflection point.

Light conditions and photosynthetic activity

The underwater light gradient is described by Lambert-Beer's law (*42*, *48*)

$$I(z) = I_{in}\exp(-K_{bg}z - kBz) \tag{2.8}$$

where $I(z)$ is the light intensity at depth z, I_{in} is the incident light intensity, K_{bg} is the background turbidity of the water itself, and k is the specific light attenuation coefficient of the cyanobacteria. We note that the light gradient changes dynamically, because the light intensity at a given depth decreases with increasing population densities B of the cyanobacteria. We define I_{out} as the light intensity reaching the bottom of the water column (i.e., $I_{out}=I(z_{max})$).

Light availability drives the light reactions of photosynthesis, and thereby the amount of energy available for carbon fixation. We calculate the relative photosynthetic activity of the cyanobacteria from the depth-averaged photosynthetic rate (*48*)

$$P = \frac{1}{z_{max}}\int_0^{z_{max}} p(I(z))dz \tag{2.9}$$

where $p(I(z))$ is the specific photosynthetic rate as a function p of the local light intensity I, which in turn is a function of depth z, and z_{max} is the total depth of the water column.

The specific photosynthetic rate is described by a simple Monod function of light intensity

$$p(I) = \frac{I}{(p_{max}/\alpha)+I} \tag{2.10}$$

where α is the initial slope of the $p(I)$ curve at I=0 and p_{max} is the maximum photosynthetic rate, which is defined as $p_{max} = V_{max,CO2,gross} + V_{max,\ HCO3}$. We note that the specific photosynthetic rate is scaled between $0 \le p(I) \le 1$, consistent with its application in equations (2.3) and (2.4).

With the Monod function in equation (2.10) and Lambert-Beer's law in equation (2.8), the depth integral in equation (2.9) can be solved analytically (*48*). This yields

$$P = \left(\frac{1}{\ln(I_{in}/I_{out})}\right)\ln\left(\frac{(p_{max}/\alpha)+I_{in}}{(p_{max}/\alpha)+I_{out}}\right) \tag{2.11}$$

DIC, alkalinity and pH

Changes in the concentration of total dissolved inorganic carbon, [DIC], are described by (*11*)

$$\frac{d[\mathrm{DIC}]}{dt} = D([\mathrm{DIC}]_{in} - [\mathrm{DIC}]) + \frac{g_{CO2}}{z_{max}} - \left(V_{CO2,gross} + V_{HCO3}\right)B + rB \qquad (2.12)$$

The first term on the right-hand side of this equation describes changes through the influx ($[\mathrm{DIC}]_{in}$) and efflux of water containing DIC. The second term describes CO_2 exchange with the atmosphere, where g_{CO2} is the CO_2 flux across the air-water interface and division by z_{max} converts the flux per unit surface area into the corresponding change in DIC concentration. The third term describes CO_2 and bicarbonate uptake by the photosynthetic activity of the cyanobacterial population, and the fourth term describes CO_2 release by respiration.

The CO_2 flux, g_{CO2}, depends on the difference in partial pressure across the air-water interface. More specifically, g_{CO2} depends on the difference between the expected concentration of dissolved CO_2 in water if it would be in equilibrium with the partial pressure in the atmosphere and the actual dissolved CO_2 concentration (*52*, *53*)

$$g_{CO2} = v(K_0 pCO_2 - [\mathrm{CO_2}]) \qquad (2.13)$$

where v is the gas transfer velocity (also known as piston velocity), K_0 is the solubility of CO_2 gas in water (also known as Henry's constant), pCO_2 is the partial pressure of CO_2 in the atmosphere, and $[CO_2]$ is the dissolved CO_2 concentration. In chemostats, gas transfer will also depend on the gas flow rate (a) and we therefore assume that $v = b\,a$, where b is a constant of proportionality.

Concentrations of dissolved CO_2, bicarbonate and carbonate can be calculated from [DIC] and pH (*45*). Changes in pH depend, in turn, on the alkalinity of water. In our application, alkalinity largely depends on the inorganic carbon and phosphate concentrations (*11*, *46*)

$$ALK = [\mathrm{HCO_3^-}] + 2[\mathrm{CO_3^{2-}}] + [\mathrm{HPO_4^{2-}}] + 2[\mathrm{PO_4^{3-}}] - [\mathrm{H_3PO_4}] + [\mathrm{OH^-}] - [\mathrm{H^+}] \qquad (2.14)$$

According to this equation, changes in dissolved CO_2 do not affect alkalinity. Furthermore, uptake of bicarbonate by phytoplankton requires the simultaneous uptake of a proton to maintain charge balance, and hence does not change alkalinity either. However, uptake of nutrients such as nitrate, phosphate and sulfate is accompanied by proton consumption to maintain charge balance and therefore increases alkalinity (*46*). Our model therefore treats alkalinity as a dynamic variable

$$\frac{dALK}{dt} = D(ALK_{in} - ALK) + (Q_N + Q_P + 2Q_S)\mu B \qquad (2.15)$$

where ALK_{in} is the alkalinity of the influx, and Q_N, Q_P and Q_S are the cellular nitrogen, phosphorus and sulfur contents of the cyanobacteria (see below). Nitrate and phosphate uptake increase alkalinity by one mole equivalent, whereas sulfate uptake increases alkalinity by 2 mole equivalents (*46*). Accordingly, although nutrients are supplied in saturating concentrations and hence do not limit cyanobacterial growth in our model and experiments, the model does keep track of the nitrate, phosphate and sulfate concentration (see below) to calculate changes in alkalinity, and hence in pH and carbon speciation.

We used an iterative algorithm adapted from Portielje and Lijklema (*54*) that, at each time step, calculates pH and the dissolved CO_2, bicarbonate and carbonate concentration from the [DIC] and alkalinity predicted by equation (2.12) and equation (2.15). The algorithm is described in the Supporting Information of (*11*).

Nutrient uptake

In our model application, nutrients do not limit cyanobacterial growth. However, the model keeps track of nutrients such as nitrate, phosphate and sulfate, because the uptake of these nutrients affects alkalinity and hence pH and carbon speciation (see above). For simplicity, we assume that the cellular carbon:nutrient stoichiometry remains constant. Hence, the cellular nitrogen, phosphorus and sulfur contents (Q_N, Q_P, Q_S) can be calculated from the cellular carbon content

$$Q_N = \frac{Q_C}{C_N}, \quad Q_P = \frac{Q_C}{C_P}, \quad Q_S = \frac{Q_C}{C_S} \tag{2.16}$$

where C_N, C_P and C_S denote the cellular C:N, C:P and C:S ratio of the cyanobacteria. Dynamic changes in the concentrations of dissolved inorganic nitrogen ([DIN]), phosphorus ([DIP]) and sulfur ([DIS]) in the chemostat depend on the influx and efflux of these nutrients and on nutrient uptake by the growing cyanobacterial population

$$\begin{aligned} \frac{d[\mathrm{DIN}]}{dt} &= D([\mathrm{DIN}]_{in} - [\mathrm{DIN}]) - \mu Q_N B \\ \frac{d[\mathrm{DIP}]}{dt} &= D([\mathrm{DIP}]_{in} - [\mathrm{DIP}]) - \mu Q_P B \\ \frac{d[\mathrm{DIS}]}{dt} &= D([\mathrm{DIS}]_{in} - [\mathrm{DIS}]) - \mu Q_S B \end{aligned} \tag{2.17}$$

where $[\mathrm{DIN}]_{in}$, $[\mathrm{DIP}]_{in}$ and $[\mathrm{DIS}]_{in}$ are the concentrations of dissolved inorganic nitrogen, phosphorus and sulfur in the influx.

Model parameterization

The model parameters consist of system parameters and species parameters. System parameters are under experimental control and were regularly measured during the experiments. We already specified several of the system parameters, such as the incident light intensity (I_{in}), pCO$_2$ level in the gas flow, and dilution rate (D) of the chemostats in the Materials and Methods section. A complete list of all system parameters is provided in Table S4.

Species parameters describe the traits of the species, in this case of *Microcystis* PCC 7806 and PCC 7941 (Table S5). Almost all species parameters were based on experimental measurements. Carbon uptake parameters ($V_{max,CO2,gross}$, $V_{max,HCO3}$, $U_{max,HCO3}$, $K_{1/2,CO2}$, $K_{1/2,HCO3}$, h) and respiration rates (r) were measured for *Microcystis* grown at low pCO$_2$ and at high pCO$_2$ using MIMS, as described in the Materials and Methods section. The cellular carbon content (Q_C) and cellular C:N, C:P and C:S ratios (C_N, C_P and C_S) were calculated from the cellular carbon, nitrogen, phosphorus and sulfur contents of *Microcystis* measured in the steady-state chemostats.

The specific light attenuation coefficient (k) of *Microcystis* and the background turbidity (K_{bg}) were estimated from the chemostat experiments performed at low and high pCO$_2$. More specifically, according to Lambert-Beer's law, equation (2.8) can be written as $\ln(I_{in}/I_{out})/z_{max} = K_{bg} + kB$. Hence, the specific light attenuation coefficient (k) was estimated as the slope of a linear regression of $\ln(I_{in}/I_{out})/z_{max}$ versus population density B, and the background turbidity (K_{bg}) was estimated as the intercept.

The initial slope α of the $p(I)$ curve at I=0 was used as 'calibration parameter' in our model. It was estimated by fitting the model predictions to the observed dynamics in the experiments using a least-squares approach. More specifically, we estimated α by fitting the time courses of population density, light transmission (I_{out}), pH, DIC, CO$_2$, bicarbonate and carbonate predicted by the model to the time courses of these variables measured in the experiments, following the same methodology as in earlier studies (*11*, *42*).

The CO$_2$ and bicarbonate uptake parameters that were significantly affected by pCO$_2$ in the experiments (Fig. 3) are considered to be plastic traits in our model. The physiological limits x_{low} and x_{high} of these plastic traits were set at the parameter values measured at low and at high pCO$_2$, respectively. The trait acclimation rate c was estimated from earlier chemostat experiments, in which *Microcystis* PCC 7806 was shifted from low to high pCO$_2$ (*33*). Since we measured the carbon uptake kinetics only for two experimental conditions (low and high pCO$_2$), we lack experimentally robust estimates of the steepness d and inflection point S of the functions f[CO$_2$] and f[HCO$_3$]. Instead, the parameters d and S were guesstimated by assuming that the shift from low-pCO$_2$ uptake kinetics to high-pCO$_2$ uptake kinetics occurred at dissolved CO$_2$ and bicarbonate concentrations somewhere halfway between the concentrations measured in the low-pCO$_2$ and high-pCO$_2$ chemostats.

The carbon uptake parameters that were not significantly affected by pCO$_2$ in the experiments (Fig. 3) were not plastic in our model. For these parameters, a constant value was used that equaled the average of the values measured in the low and high pCO$_2$ experiments.

Sensitivity analysis

We performed a sensitivity analysis to assess how variation in the value of the calibration parameter α would affect the model predictions. The normalized sensitivity coefficient (*SC*) is a local sensitivity index that quantifies the relative change in model output *Y* in response to a relative change in input parameter *Z* (*11*, *55*)

$$SC = \frac{(\Delta Y / Y)}{(\Delta Z / Z)} \tag{2.18}$$

We based the calculation of *SC* on the change in the predicted population density at steady state in response to a 1% increment of α. $|SC| >> 1$ indicates that the model predictions are very sensitive to a change in α, whereas $|SC| << 1$ indicates that they are rather insensitive. The results show that the model predictions were insensitive to variation in α at low $p\mathrm{CO_2}$ (*SC* = 0.056 for PCC 7806 and *SC* = 0.012 for PCC 7941), but more sensitive to variation in α at high $p\mathrm{CO_2}$ (*SC* = 0.64 for PCC 7806 and *SC* = 0.66 for PCC 7941). This is in line with expectation, as it indicates that the population dynamics of *Microcystis* are sensitive to variation in the initial slope of the $p(I)$ curve when growth is light-limited (at high $p\mathrm{CO_2}$) but not when growth is carbon-limited (at low $p\mathrm{CO_2}$).

Section S3. Extrapolation of the model to lakes

Introduction and approach

The chemostat systems in which we cultured *Microcystis* are designed to carry out experiments and test model predictions under highly controlled conditions in the laboratory. Natural systems, however, function at larger temporal and spatial scales, and are more complex than our small-scale laboratory experiments. Here, we describe how we extended and adapted our model to bear more semblance to cyanobacterial bloom dynamics in lakes (*11*). We do not aim at a model that describes the detailed spatial and temporal development of a specific *Microcystis* bloom in a specific lake. Instead, our aim is to develop a generic model that captures the main features of *Microcystis* blooms, to gain an improved understanding of how acclimation of the carbon uptake kinetics as observed in our experiments may modify the response of *Microcystis* blooms to rising atmospheric pCO_2.

For this purpose, we up-scale the dimensions of the model from the laboratory chemostat to lake dimensions and include additional loss processes of the cyanobacterial population (e.g., by grazing or viruses). Similar to the chemostat experiments, we assume eutrophic conditions to assure that *Microcystis* bloom development is not limited by nutrients but primarily controlled by the availability of inorganic carbon and light. In addition, we include (partial) mineralization of the carbon and nutrient contents of dead cyanobacteria. Furthermore, we include the impact of chemical enhancement, the additional influx of atmospheric CO_2 into waters of high pH caused by the reaction of CO_2 with hydroxide ions (*15*, *56*).

Model description

To model *Microcystis* blooms in lakes, we use a similar model structure as for the chemostats (section S2). However, we make the following changes:

Up-scaling: We adapt our model system from a small laboratory chemostat to a eutrophic lake with a mixing depth of 7 m. The high background turbidity of the chemostat is reduced to a lower background turbidity of a lake. The low incident light intensity (I_{in}) of 40 μmol photons m^{-2} s^{-1} in the chemostat is replaced by a much higher incident light intensity of 400 μmol photons m^{-2} s^{-1} in the lake. The high dilution rate of the chemostat is replaced by a low turnover rate, representing a lake with a residence time of 100 days. The low alkalinity in the chemostat is replaced by the wide range of alkalinities observed in lakes. The very high phosphate and nitrate concentrations in the mineral medium of the chemostat are diminished to a lower (but still fairly high) phosphate concentration of 4 μmol L^{-1} and nitrate concentration of 160 μmol L^{-1} representative for eutrophic lakes dominated by cyanobacterial blooms (*57*, *58*).

Population dynamics: In the chemostats, we assumed that *Microcystis* losses were dominated by the dilution rate. In lakes, cyanobacteria are exposed to many other loss factors, such as sedimentation, grazing by zooplankton and viral lysis. We therefore included an additional loss factor. Let *B* denote the population density of *Microcystis*. The population dynamics can then be described by the following equation

$$\frac{dB}{dt} = (\mu - D - m)B \quad (3.1)$$

where μ is the specific growth rate of *Microcystis* as function of inorganic carbon and light availability, *D* is the low turnover rate of the lake (i.e., the inverse of the residence time), and *m* is the specific mortality rate of *Microcystis* due to, e.g., sedimentation, zooplankton or viruses.

We assume that the specific growth rate of *Microcystis* is governed by the carbon balance, which again depends on the photosynthetic uptake of CO_2 and bicarbonate and on losses of CO_2 by respiration. Hence, the specific growth rate is formulated similarly as before, as described by equations (2.2) - (2.11) in section S2.

Carbon and nutrient recycling: In chemostats, inorganic carbon and nutrients are supplied by the gas flow and the influx of mineral medium, while organic carbon and nutrients contained in cyanobacterial cells are washed out by dilution and lost. In contrast, dead phytoplankton in lakes is often mineralized, which recycles carbon and nutrients from dead organic matter into the inorganic carbon and nutrient pools. For simplicity, we assume that recycling of dead material is instantaneous, so that the carbon and nutrient contents of dead cyanobacteria immediately enter the DIC and nutrient pools. However, we assume that the recycling efficiency is less than 100%. That is, a fraction ε of the dead cyanobacteria is recycled, whereas a fraction 1-ε is permanently lost from the water column, for instance by burial in the sediment. We assumed a recycling efficiency of ε = 0.95.

The dynamics of dissolved inorganic nitrogen, phosphorus and sulfur can therefore be described as follows

$$\begin{aligned} \frac{d[\mathrm{DIN}]}{dt} &= D([\mathrm{DIN}]_{in} - [\mathrm{DIN}]) - \mu Q_N B + \varepsilon m Q_N B \\ \frac{d[\mathrm{DIP}]}{dt} &= D([\mathrm{DIP}]_{in} - [\mathrm{DIP}]) - \mu Q_P B + \varepsilon m Q_P B \\ \frac{d[\mathrm{DIS}]}{dt} &= D([\mathrm{DIS}]_{in} - [\mathrm{DIS}]) - \mu Q_S B + \varepsilon m Q_S B \end{aligned} \quad (3.2)$$

These equations are identical to equations (2.17) in section S2, but include an additional term representing the mineralization rates of nutrients from dead *Microcystis* cells.

Similarly, changes in dissolved inorganic carbon, DIC, are described by the following equation

$$\frac{d[\mathrm{DIC}]}{dt} = D([\mathrm{DIC}]_{in} - [\mathrm{DIC}]) + \frac{g_{CO2}}{z_{max}} - \left(V_{CO2,gross} + V_{HCO3}\right)B + rB + \varepsilon m Q_C B \quad (3.3)$$

This equation is identical to equation (2.12) in section S2, but also includes the mineralization rate of organic carbon from dead *Microcystis*.

Uptake of nitrate, phosphate and sulfate by cyanobacteria increases alkalinity, whereas mineralization of these nutrients decreases alkalinity (*46*). Hence, dynamic changes in alkalinity can be described as

$$\frac{dALK}{dt} = D(ALK_{in} - ALK) + (Q_N + Q_P + 2Q_S)\mu B - \varepsilon(Q_N + Q_P + 2Q_S)mB \quad (3.4)$$

This equation is identical to equation (2.15) in section S2, but also includes effects of nutrient mineralization on alkalinity.

Gas flux across the air-water interface: Similar to the chemostat experiments, we assume that the CO_2 gas flux across the air-water interface is proportional to the difference between the expected concentration of dissolved CO_2 in water if it would be in equilibrium with the atmosphere (calculated from Henry's law) and the actual concentration of dissolved CO_2 (*52*, *53*). At high pH, the CO_2 influx is further augmented by the reaction $CO_2 + OH^- \leftrightarrow HCO_3^-$, which removes CO_2 and thereby ensures a steeper CO_2 concentration gradient in the boundary layer (*15*, *56*). This augmented CO_2 influx is commonly known as chemical enhancement, and represented by the chemical enhancement factor β

$$g_{CO2} = v\beta(K_0 pCO_2 - [\mathrm{CO_2}]) \quad (3.5)$$

where v is the gas transfer velocity (also known as piston velocity) across the air-water interface, K_0 is the solubility constant of CO_2 gas in water, and pCO$_2$ is the partial pressure of CO_2 in the atmosphere. The gas transfer velocity depends on several parameters, especially wind speed. A typical value for the gas transfer velocity of lakes is v= 0.0185 m h^{-1} (*56*, *59*). The chemical enhancement factor β can vary from a baseline value of 1 for pH < 5, but may rise exponentially to values of 4 to 8 for pH > 9 (*56*).

Similar to previous studies (*15*, *56*), the chemical enhancement factor was calculated as

$$\beta = \frac{\tau}{(\tau-1)+\tanh\left\{\left(\frac{\rho\tau}{D_m}\right)^{0.5} z\right\} \Big/ \left\{\left(\frac{\rho\tau}{D_m}\right)^{0.5} z\right\}} \quad (3.6)$$

where D_m is the molecular diffusivity and z is the thickness of the stagnant boundary layer, which is equal to D_m/g_{CO2}. The parameter τ is defined as

$$\tau = \frac{[\mathrm{H^+}]^2}{K_1K_2 + K_1[\mathrm{H^+}]} + 1 \quad (3.7)$$

where K_1 and K_2 are the equilibrium constants describing the reactions $CO_2 + H_2O \leftrightarrow HCO_3^- + H^+$, and $HCO_3^- \leftrightarrow CO_3^{2-} + H^+$, respectively. Finally, ρ is the combined rate of the forward reactions of CO_2 with H_2O and OH^-

$$\rho = k_{CO2} + k_{OH}[OH^-] \quad (3.8)$$

where k_{CO2} is the rate of the forward reaction $CO_2 + H_2O \rightarrow HCO_3^- + H^+$, and k_{OH} is the rate of the forward reaction $CO_2 + OH^- \rightarrow HCO_3^-$.

Model parameterization

We choose parameter values representative for the summer situation in eutrophic and hypertrophic lakes dominated by dense blooms of the cyanobacterium *Microcystis*. The species parameters are identical to those of *Microcystis* PCC 7806 measured in our chemostat experiments (Table S5). System parameters specific for the lake model are summarized in Table S6.

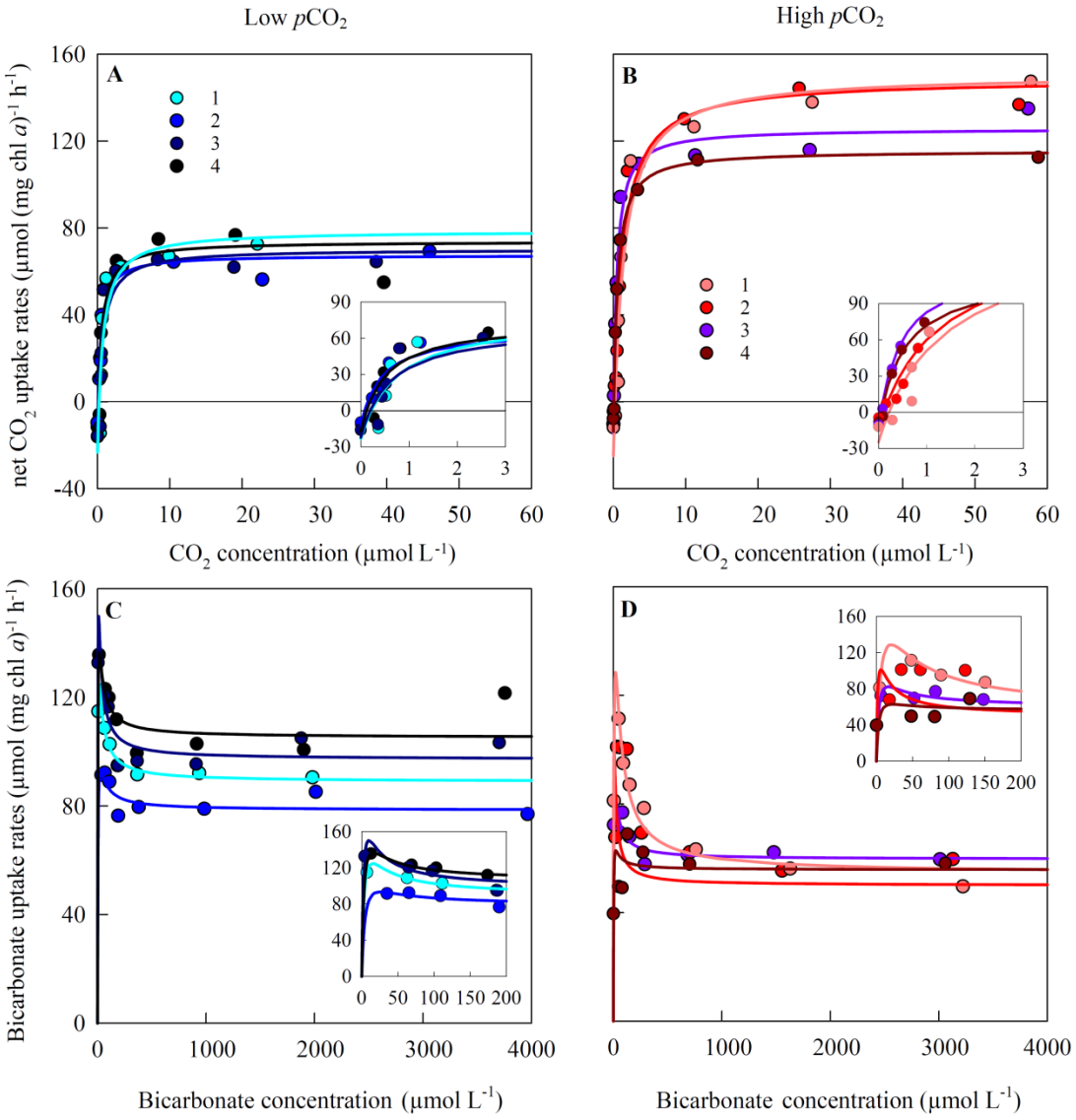

Fig. S1. Carbon uptake kinetics of *Microcystis* PCC 7941 acclimated to either low or high pCO_2. (**A** and **B**) Net CO_2 uptake rate as function of the dissolved CO_2 concentration, after acclimation to (A) low pCO_2 and (B) high pCO_2. (**C** and **D**) Bicarbonate uptake rate as function of the bicarbonate concentration, after acclimation to (C) low pCO_2 and (D) high pCO_2. Carbon uptake kinetics were measured after ~20 days of acclimation to the steady-state conditions in the chemostats. Measurements were replicated fourfold, as indicated by the different colors. Lines are Michaelis-Menten fits to each of the replicates (see section S1 for our modified bicarbonate uptake model and Table S2 for parameter estimates). Insets zoom in at the carbon uptake kinetics at low dissolved CO_2 and bicarbonate concentrations.

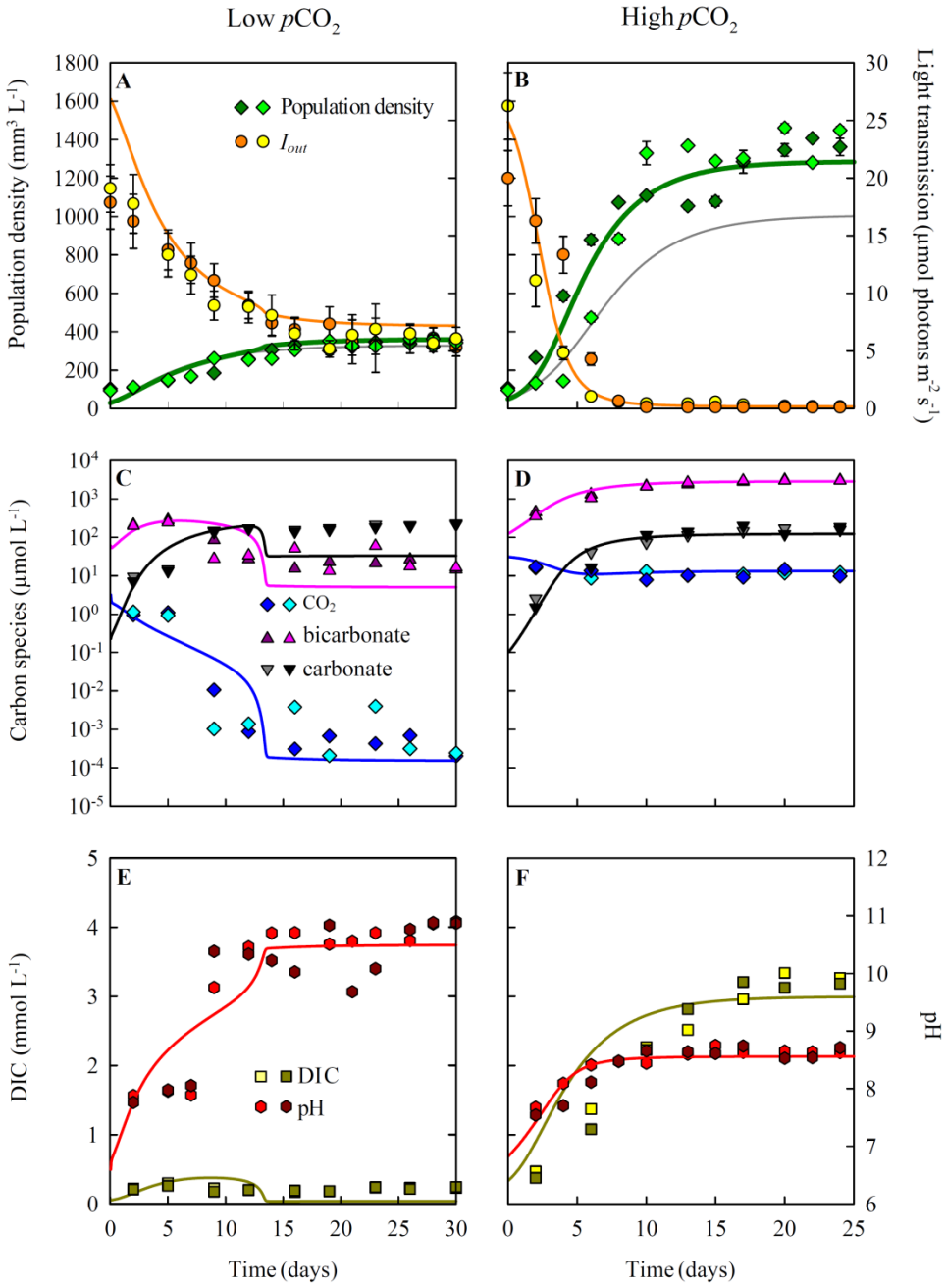

Fig. S2. Population density, inorganic carbon chemistry, and pH in chemostat experiments with *Microcystis* PCC 7941 at low and at high pCO_2. Chemostat experiments were performed in duplicate, at low pCO_2 (left panels) and at high pCO_2 (right panels). (**A** and **B**) *Microcystis* population density (n=3 technical replicates per chemostat) and light transmission I_{out} (n=10) through the chemostat. (**C** and **D**) Dissolved CO_2, bicarbonate and carbonate concentrations. (**E** and **F**) Dissolved inorganic carbon (DIC) and pH (n=3 technical replicates per chemostat). Symbols indicate experimental data of the duplicate chemostat experiments, error bars indicate standard deviations (SD) of technical replicates, and lines indicate model predictions. Error bars in (E) and (F) did not exceed the size of the symbols. For comparison, gray lines in (A) and (B) are model predictions for non-acclimated cells, that either (A) grow at low pCO_2 but with carbon uptake kinetics acclimated to high pCO_2, or (B) grow at high pCO_2 but with carbon uptake kinetics acclimated low pCO_2. Steady-state characteristics of the experiments are summarized in Table S1 and parameter values of the model are listed in Tables S4 and S5.

Table S1. Steady-state characteristics of the chemostat experiments with *Microcystis* PCC 7806 and *Microcystis* PCC 7941. Steady-state values were calculated as average values ± SD of the *n*=3-5 consecutive data points measured towards the end of the chemostat experiments.

Parameter	Low pCO_2	High pCO_2
***Microcystis aeruginosa* PCC 7806**		
Population density ($mm^3\ L^{-1}$)	459 ± 33	1041 ± 58
Light penetration (µmol photons $m^{-2}\ s^{-1}$)	4.1 ± 1.0	0.2 ± 0.0
pH	11.1 ± 0.0	8.7 ± 0.2
Dissolved inorganic carbon (µmol L^{-1})	130 ± 44	3062 ± 254
Dissolved CO_2 concentration (µmol L^{-1})	0.00012 ± 0.00004	14.2 ± 1.1
Bicarbonate concentration (µmol L^{-1})	8.5 ± 2.7	2926.7± 240.2
Carbonate concentration (µmol L^{-1})	121.0 ± 41.4	121.2 ± 12.8
Cell size (μm^3)	23.3 ± 1.0	25.2 ± 1.4
Cellular Chl *a* content (pg $cell^{-1}$)	0.12 ± 0.00	0.17 ± 0.01
***Microcystis aeruginosa* PCC 7941**		
Population density ($mm^3\ L^{-1}$)	341 ± 11	1397 ± 35
Light penetration (µmol photons $m^{-2}\ s^{-1}$)	6.0 ± 0.2	0.1 ± 0.0
pH	10.8 ± 0.3	8.6 ± 0.1
Dissolved inorganic carbon (µmol L^{-1})	233 ± 8	3182 ± 85
Dissolved CO_2 concentration (µmol L^{-1})	0.00097 ± 0.00107	11.5 ± 1.7
Bicarbonate concentration (µmol L^{-1})	26.1 ± 13.0	3007.4 ± 152.8
Carbonate concentration (µmol L^{-1})	206.8 ± 12.6	158.6 ± 14.9
Cell size (μm^3)	81.1 ± 4.4	35.0 ± 1.1
Cellular Chl *a* content (pg $cell^{-1}$)	0.28 ± 0.11	0.19 ± 0.03

Table S2. Kinetic parameters estimated from the carbon uptake experiments with *Microcystis* PCC 7806 and *Microcystis* PCC 7941. Carbon uptake kinetics were measured after ~20 days of acclimation to steady-state conditions at either low pCO_2 or high pCO_2. The carbon uptake kinetics were replicated three or four times per pCO_2 treatment. Kinetic parameters were estimated by fitting Michaelis-Menten equations to each replicate (Fig. 2 and Fig. S1). For the bicarbonate uptake of *Microcystis* PCC 7941 we used a variant of the Michaelis-Menten equation with an additional parameter *h* to capture the asymptotic decrease of the bicarbonate uptake rate at high bicarbonate concentrations (see section S1 for details).

Assay	Net CO_2 uptake		Bicarbonate uptake			Respiration
***Microcystis aeruginosa* PCC 7806**						
Acclimated to low pCO_2						
	$V_{max,CO2,net}$	$K_{1/2,CO2}$	$V_{max,HCO3}$	$K_{1/2,HCO3}$		r
1	21.6	0.40	122.1	3.01		15.0
2	26.2	0.76	116.4	6.52		12.7
3	22.2	0.20	101.8	5.68		7.2
4	23.2	0.23	108.4	4.79		10.0
mean	23.3	0.40	112.2	5.00		11.2
Acclimated to high pCO_2						
1	120.1	1.50	94.5	14.46		15.7
2	119.0	1.62	101.1	11.04		7.4
3	115.5	1.80	113.2	10.69		10.9
mean	118.2	1.64	102.9	12.06		11.3
***Microcystis aeruginosa* PCC 7941**						
Acclimated to low pCO_2						
	$V_{max,CO2,net}$	$K_{1/2,CO2}$	$U_{max,HCO3}$	$K_{1/2,HCO3}$	h	r
1	78.7	0.72	293.5	8.04	0.30	23.2
2	67.5	0.42	182.1	10.46	0.43	12.3
3	70.2	0.60	380.4	5.89	0.26	22.1
4	73.7	0.49	299.3	7.64	0.35	17.4
mean	72.5	0.56	288.8	8.01	0.34	18.7
Acclimated to high pCO_2						
1	150.8	1.31	397.5	15.63	0.14	24.8
2	148.5	1.20	295.1	4.48	0.17	13.3
3	125.7	0.44	190.9	8.45	0.31	14.8
4	129.3	0.51	111.9	7.48	0.50	14.3
mean	133.9	0.87	248.9	9.01	0.28	16.8

Units for V_{max}, U_{max} and r are µmol C (mg chl a)$^{-1}$ h^{-1}; units for $K_{1/2}$ are µmol L^{-1}; h is dimensionless.

Table S3. Tests of significant differences between kinetic parameters estimated at low versus high pCO_2. Parameter values are given as mean ± SD based on n=3-4 assays per pCO_2 treatment. Significant differences between parameter values are assessed with an independent-samples t-test, corrected for multiple hypothesis testing using the false discovery rate (*44*).

Parameter		Low pCO_2	High pCO_2	t-test	p
***Microcystis aeruginosa* PCC 7806**					
CO_2 uptake	$V_{max,CO2,net}$	23.3 ± 2.1	118.2 ± 2.4	t_5=56.5	< 0.001
	$V_{max,CO2,gross}$	34.5 ± 4.1	129.5 ± 5.4	t_5=26.7	< 0.001
	$K_{1/2,CO2}$	0.40 ± 0.26	1.64 ± 0.15	t_5=7.4	< 0.05
HCO_3^- uptake	$V_{max,\ HCO3}$	112.2 ± 8.9	102.9 ± 9.5	t_5=−1.3	n.s.
	$K_{1/2,\ HCO3}$	5.00 ± 1.50	12.06 ± 2.08	t_5=5.3	< 0.05
Respiration	r	11.2 ± 3.3	11.3 ± 4.1	t_5=0.0	n.s.
***Microcystis aeruginosa* PCC 7941**					
CO_2 uptake	$V_{max,CO2,net}$	72.5 ± 4.8	133.9 ± 19.3	t_6=6.2	< 0.05
	$V_{max,CO2,gross}$	91.3 ± 9.1	150.7 ± 22.5	t_6=5.3	< 0.05
	$K_{1/2,CO2}$	0.56 ± 0.13	0.85 ± 0.47	t_6=1.3	n.s.
HCO_3^- uptake	$V_{max,HCO3}$	92.4 ± 11.5	54.9 ± 3.96	t_6=6.2	< 0.05
	$K_{1/2,HCO3}$	8.01 ± 1.88	9.02 ± 4.72	t_6=0.4	n.s.
Respiration	r	18.7 ± 5.0	16.8 ± 5.4	t_6=0.5	n.s.

Units for V_{max} and r are µmol C (mg chl a)$^{-1}$ h^{-1}; units for $K_{1/2}$ are µmol L^{-1}.

Table S4. System parameters applied in the chemostat experiments.

Parameter	Description	Value	Units
D	Dilution rate	0.2	d^{-1}
I_{in}	Incident light intensity	40	µmol photons m^{-2} s^{-1}
K_{bg}	Background turbidity	5.5	m^{-1}
z_m	Mixing depth	0.05	m
pCO_2	Partial pressure of CO_2 in the gas flow	100 or 1,000	ppm
$[DIC]_{in}$	DIC concentration at influx	0	µmol L^{-1}
$[DIN]_{in}$	Nitrate concentration at influx	8,000	µmol L^{-1}
$[DIP]_{in}$	Phosphate concentration at influx	175	µmol L^{-1}
$[DIS]_{in}$	Sulfate concentration at influx	300	µmol L^{-1}
ALK_{in}	Alkalinity at influx	175	µEq L^{-1}
T	Temperature	25	^oC
Sal	Salinity	0.85	g L^{-1}
a	Gas flow rate	30	L h^{-1}
b	Constant of proportionality for gas transfer across the air-water interface	0.23 - 0.60	L^{-1}

Table S5. Species parameters measured experimentally.

Parameter	Description	PCC 7806	PCC 7941	Units
$V_{max,CO2,gross}$	Maximum gross uptake rate of CO_2	4.4 – 21.1[(a)]	8.4 – 21.1[(a)]	µmol C mm^{-3} d^{-1} [(b)]
$V_{max,HCO3}$	Maximum bicarbonate uptake rate	15.4	-	µmol C mm^{-3} d^{-1} [(b)]
$U_{max,HCO3}$	Hypothetical maximum bicarbonate uptake rate	-	26.7 – 36.1[(a)]	µmol C mm^{-3} d^{-1} [(b)]
h	Fraction of hypothetical maximum bicarbonate uptake rate realized at saturating bicarbonate concentrations	-	0.28 – 0.34[(a)]	-
$K_{1/2,CO2}$	Half-saturation constant for CO_2	0.40 – 1.64[(a)]	0.71	µmol L^{-1}
$K_{1/2,HCO3}$	Half-saturation constant for HCO_3^-	5.0 – 12.1[(a)]	8.5	µmol L^{-1}
r	Respiration rate	1.6	2.0	µmol C mm^{-3} d^{-1} [(b)]
α	initial slope of the $p(I)$ curve at I=0	1.05[(c)]	1.20[(c)]	µmol C (µmol photons m^{-2} s^{-1})$^{-1}$ mm^{-3} d^{-1}
k	Specific light attenuation coefficient	1.0×10^{-4}	0.8×10^{-4}	m^2 mm^{-3}
Q_C	Cellular carbon content	15.7	15.7	µmol C mm^{-3}
C_N	Cellular C:N ratio	5.4	7.7	(molar ratio)
C_P	Cellular C:P ratio	97	125	(molar ratio)
C_S	Cellular C:S ratio	182	250	(molar ratio)
c	Trait acclimation rate	1.0	1.0	d^{-1}
d_{CO2}	Slope of the logistic curve describing the reaction norm for CO_2-specific parameters	3.5	3.5	-
d_{HCO3}	Slope of the logistic curve describing the reaction norm for HCO_3^--specific parameters	6.0	6.0	-
S_{CO2}	CO_2 concentration at which the trait value is exactly between its minimum and maximum	1.0	1.0	µmol CO_2 L^{-1}
S_{HCO3}	HCO_3 concentration at which the trait value is exactly between its minimum and maximum	316	1000	µmol HCO_3^- L^{-1}

[(a)] Parameter range of plastic trait, from x_{low} to x_{high}.
[(b)] Units were converted from µmol C (mg Chl *a*)$^{-1}$ h^{-1} to µmol C mm^{-3} d^{-1} using the cellular Chl *a* content and cell size reported in Table S1.
[(c)] The parameter values of α were estimated by calibrating the model predictions to the time courses of the experiments.

Table S6. System parameters applied in the lake model.

Parameter	Description	Values	Units
D	Lake turnover rate	0.01	d^{-1}
m_i	Specific mortality rate	0.01	d^{-1}
I_{in}	Incident light intensity	400	µmol photons m^{-2} s^{-1}
K_{bg}	Background turbidity	0.6	m^{-1}
z_m	Mixing depth	7.0	m
$p\mathrm{CO_2}$	Partial pressure of atmospheric CO_2	1 – 1,600	ppm
$[\mathrm{DIC}]_{in}$	DIC concentration at influx	100 – 10,000[(a)]	µmol L^{-1}
ALK_{in}	Alkalinity at influx	100 – 10,000[(a)]	µEq L^{-1}
$[\mathrm{DIN}]_{in}$	Nitrate concentration at influx	160	µmol L^{-1}
$[\mathrm{DIP}]_{in}$	Phosphate concentration at influx	4	µmol L^{-1}
$[\mathrm{DIS}]_{in}$	Sulfate concentration at influx	6	µmol L^{-1}
ε	Nutrient recycling efficiency	0.95	-
T	Temperature	20	^{o}C
Sal	Salinity	0.142	g L^{-1}
v	Piston velocity	0.0185	m h^{-1}
D_m	Molecular diffusion coefficient	1.68×10^{-9}	m^2 s^{-1}
k_{CO2}	Forward rate of CO_2 reacting with H_2O	2.38×10^{-2}	s^{-1}
k_{OH}	Forward rate of CO_2 reacting with OH^-	3454	mol^{-1} s^{-1}

[(a)] In our lake model, ALK_{in} was a set parameter and $[\mathrm{DIC}]_{in}$ was calculated from ALK_{in} and $[\mathrm{DIP}]_{in}$.